

# PVDF-*g*-PSSA and Al<sub>2</sub>O<sub>3</sub> composite proton exchange membranes

Yi Shen, Xinping Qiu\*, Juan Shen, Jingyu Xi, Wentao Zhu

*Key Laboratory of Organic Optoelectronics and Molecular Engineering, Department of Chemistry, Tsinghua University, Beijing 100084, China*

Received 11 January 2006; received in revised form 21 March 2006; accepted 28 March 2006

Available online 6 May 2006

## Abstract

Poly(vinylidene fluoride) grafted polystyrene sulfonated acid (PVDF-*g*-PSSA) membranes doped with different amount of Al<sub>2</sub>O<sub>3</sub> (PVDF/Al<sub>2</sub>O<sub>3</sub>-*g*-PSSA) were prepared based on the solution-grafting technique. The microstructure of the membranes was characterized by IR-spectra and scanning electron microscope (SEM). The thermal stability was measured by thermal gravity analysis (TGA). The degree of grafting, water-uptake, proton conductivity and methanol permeability were measured. The results show that the PVDF-*g*-PSSA membrane doped with 10% Al<sub>2</sub>O<sub>3</sub> has a lower methanol permeability of  $6.6 \times 10^{-8} \text{ cm}^2 \text{ s}^{-1}$ , which is almost one-fortieth of that of Nafion-117, and this membrane has moderate proton conductivity of  $4.5 \times 10^{-2} \text{ S cm}^{-1}$ . Tests on cells show that a DMFC with the PVDF/10%Al<sub>2</sub>O<sub>3</sub>-*g*-PSSA has a better performance than Nafion-117. Although Al<sub>2</sub>O<sub>3</sub> has some influence on the stability of the membrane, it can still be used in direct methanol fuel cells in the moderate temperature.

© 2006 Elsevier B.V. All rights reserved.

*Keywords:* Proton exchange membrane; PVDF-*g*-PSSA; Nano-Al<sub>2</sub>O<sub>3</sub>

## 1. Introduction

In recent years, the direct methanol fuel cell (DMFC) has attracted more and more attention due to its potential applications in portable electronics and vehicles. Normally, the widely used membranes in DMFC are still perfluorinated membranes, such as Nafion membranes, due to their excellent proton conductivity and high stability; however, high methanol permeability and cost are the main obstacles for using this kind of membrane in DMFC.

In order to improve the performance of proton exchange membranes, some new membranes were investigated to substitute for the perfluorinated membranes, such as polybenzimidazole (BPO) [1–4], poly(arylene ether sulfone) [5], poly(ether-ether-ketone) [6,7], sulfonated polysulfone [8]; much work has focused on amelioration the existing membrane. Kadirgan and Savadogo [9] reduced the methanol permeability by modifying the surface of the Nafion membrane with a film of poly(methyl pyrrole) by an electrochemical method;

Miyake et al. [10] and Jung et al. [11] modified a Nafion membrane with nano-SiO<sub>2</sub> to improve its affinity for water and restrain methanol crossover; Panero et al. [12] prepared polyelectrolyte by swelling a ceramic-added composite PVDF poly(vinylidene fluoride)-based membrane in a H<sub>3</sub>PO<sub>4</sub> solution. Mauritz et al. [13] reported a novel Nafion/silica hybrid membrane, and suggested the –OH on the surface of silica nano-particles can enhance the hydrophilicity of clusters inside the membranes and improve the proton conductivity at elevated temperatures.

PVDF is a kind of partial fluorinated polymer with excellent stability and has been widely used in the battery field [14–17]. It is also used for preparation of proton exchange membranes. Scrosati and co-workers [18] reported a kind of membrane based on PVDF by doping with a microporous ceramic. Lehtinen et al. [19] prepared poly(vinylidene fluoride) grafted polystyrene sulfonated acid (PVDF-*g*-PSSA) proton exchange membranes based on a radiation-grafting technique, and they found that PVDF-*g*-PSSA membranes have a higher proton conductivity, water-uptake and lower oxygen solution ability compared to Nafion membranes.

Our lab has reported a method of preparing a PVDF-*g*-PSSA membrane based on a solution-grafting technique [20]. The

\* Corresponding author. Tel.: +8610 62794234; fax: +8610 62794234.  
E-mail address: [qiuxp@mail.tsinghua.edu.cn](mailto:qiuxp@mail.tsinghua.edu.cn) (X. Qiu).

membranes prepared with this method showed a higher proton conductivity and a much lower methanol permeability. In this paper, nano- $\text{Al}_2\text{O}_3$  was doped into the PVDF before the grafting reaction; the water-uptake, proton conductivity and methanol permeability were measured, and the structure of the membranes was characterized by IR-spectra and scanning electron microscope (SEM).

## 2. Experimental

### 2.1. Membrane preparation

Nano- $\text{Al}_2\text{O}_3$  (>99.99%, Zhou Shan MingRi Company, China, average size  $30 \pm 5$  nm) and PVDF powders (ShanAi FuXing Company, ShangHai,  $M=2 \times 10^5$ ) were dispersed in a *N*-methyl pyrrolidinone (NMP) solvent by intensely stirring to obtain a homogeneous slurry which was then cast onto a glass substrate. After heating at  $80^\circ\text{C}$  for 4 h to remove NMP, the PVDF- $\text{Al}_2\text{O}_3$  composite membrane was obtained. The weight content of  $\text{Al}_2\text{O}_3$  was controlled to be 2, 5, 10, 15, 20 and 25%, respectively. For comparison, some PVDF membranes with no  $\text{Al}_2\text{O}_3$  were also prepared with the same process.

The grafting reactions were carried out with the method described in literature [20]. Firstly, the composite membrane was treated in 0.5 M KOH alcohol solution at  $80^\circ\text{C}$  for 12 h to form free radicals in the PVDF chains and the membrane was washed in deionized water. The treated membrane was then immersed in styrene and tetrahydrofuran (THF) mixed solvent (5:1, v/v). Benzoyl peroxide (BPO), with a concentration of  $3 \times 10^{-3} \text{ g ml}^{-1}$  was used as the radical initiator. The grafting reaction was performed at  $80^\circ\text{C}$  for 12 h under a nitrogen atmosphere; after grafting, the membrane was extracted with chloroform for 48 h to remove the unreacted monomer and homopolymer; finally, the membrane was sulfonated in sulfuric acid (98%) for 6 h at  $70^\circ\text{C}$  after swelling in the 1,2-dichloroethane at  $80^\circ\text{C}$  for 3 h. The membrane was then washed with deionized water to remove the remaining sulfuric acid. According to the content of  $\text{Al}_2\text{O}_3$ , we denoted the membranes as PVDF/ $x\text{Al}_2\text{O}_3$ -g-PSSA ( $x$  was the weight percent of  $\text{Al}_2\text{O}_3$  in the membranes).

### 2.2. Membrane characterization

The Fourier transform infrared (FT-IR) spectra of the membranes were collected on a Perkin-Elmer infrared spectrophotometer (Spectrum GX) in the frequency range of  $4000\text{--}500 \text{ cm}^{-1}$ . The thermal gravity analysis (TGA) was carried out by a Universal V5.3 C 2050 Instrument under the nitrogen atmosphere, and the samples were heated from  $40^\circ\text{C}$  to  $500^\circ\text{C}$  at a rate of  $20^\circ\text{C min}^{-1}$ . The morphology of the surface and cross-section of the membranes PVDF/10% $\text{Al}_2\text{O}_3$ -g-PSSA and PVDF-g-PSSA were observed on scanning electron microscope (SEM LEO-1530). Cross-sections of the samples were obtained by freezing the samples in the liquid nitrogen and rupturing them as soon as possible. Before the observation, the gold was sputtered onto the surface and cross-section of the membranes.

### 2.3. The degree of grafting

The degree of grafting (d.o.g) was determined gravimetrically according to Eq. (1):

$$\text{d.o.g} = \frac{M_1 - M_0}{M_0} \times 100\% \quad (1)$$

where  $M_0$  is the mass of the initial membrane and  $M_1$  is the mass of the polystyrene-grafted membrane. Before the measurement, membranes were dried in a vacuum oven at  $100^\circ\text{C}$  for 8 h.

### 2.4. Water-uptake

The water-uptake of the membranes was defined as the ratio of the mass of the absorbed water to that of the dry membrane. It can be calculated from Eq. (2):

$$\text{Water-uptake} = \frac{W_1 - W_0}{W_0} \quad (2)$$

where  $W_1$  is the weight of the wet membrane and  $W_0$  is the weight of the dry membrane.

### 2.5. Proton conductivity

Proton conductivity of the membranes was determined by measuring the impedance spectroscopy on a cell with the given membrane sample sandwiched between two stainless steel (SS) electrodes. The measurements were carried out on a Solartron 1255B frequency response analyzer coupled with a Solartron 1287 electrochemical interface in the frequency range of 1 Hz to 1 MHz. The conductivity was calculated according to the electrode area of the cell ( $0.785 \text{ cm}^2$ ) and the thickness of the membrane. Before each measurement was carried out, the membrane was equilibrated in deionized water for 12 h at ambient temperature. The measurements of conductivity at high temperature were carried out in an oven.

### 2.6. Methanol permeability

A two-reservoir polymethyl methacrylate cell, as described in literature [20], was used to measure the methanol permeability of the membranes. The left reservoir was filled with an aqueous solution of methanol (30 mass%), while the right reservoir was filled with deionized water. The two reservoirs had a circularly symmetrical transport channel with the membrane clamped between them. The methanol flux was established because of the difference between the two reservoirs. The change of the methanol concentration of the right reservoir was determined by a gas chromatograph (GC-14C).

### 2.7. Fuel cell performance

Membrane electrode assemblies (MEA) with a geometric area of  $4.0 \text{ cm}^2$  were prepared using PtRu/Vulcan XC-72 and Pt/Vulcan XC-72 as the cathode and anode catalysts, respectively, each at a loading of  $3.0 \text{ mg cm}^{-2}$ . MEA inks were prepared as follows: 40 mg catalyst and 200 mg 10 wt% Nafion

solution were mixed thoroughly with 200 mg isopropyl alcohol. Inks were painted onto single sided supporting carbon paper, followed by solvent drying at 80 °C. The MEAs were obtained by hot-pressing the anode and cathode on both sides of the pre-treated membranes under 130 °C and 9 atm for 3 min.

Tests on the DMFC were performed with a cell with a cross-sectional area of 4 cm<sup>2</sup>. Different methanol solution was supplied by a pump with a rate of 2 ml min<sup>-1</sup>, and the oxygen was supplied from cylinders at ambient temperature and pressure with a rate of 200 ml min<sup>-1</sup>.

### 3. Results and discussion

#### 3.1. Morphology

The morphology of the surfaces and the cross-sections of the PVDF-*g*-PSSA membrane and PVDF/10%Al<sub>2</sub>O<sub>3</sub>-*g*-PSSA membrane are shown in Fig. 1. It can be seen that the membranes are compact and there are no penetrable holes in the membranes, which is consistent with low methanol permeability.

#### 3.2. FT-IR spectra

Fig. 2 shows the FT-IR spectra of PVDF, PVDF/10%Al<sub>2</sub>O<sub>3</sub>, PVDF-*g*-PSSA and the PVDF/10%Al<sub>2</sub>O<sub>3</sub>-*g*-PSSA membrane. It can be seen that four additional peaks, 3450, 1650, 1038 and

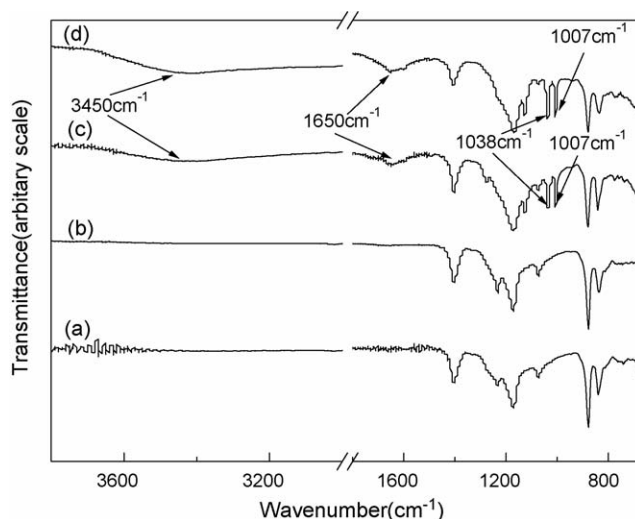


Fig. 2. The IR-spectra of: (a) PVDF membrane, (b) PVDF/10%Al<sub>2</sub>O<sub>3</sub> membrane, (c) PVDF/10%Al<sub>2</sub>O<sub>3</sub>-*g*-PSSA membrane and (d) PVDF-*g*-PSSA membrane.

1007 cm<sup>-1</sup>, were found in the spectra for PVDF-*g*-PSSA and PVDF/10%Al<sub>2</sub>O<sub>3</sub>-*g*-PSSA membrane. The peak at 1007 cm<sup>-1</sup> corresponds to the symmetrically vibration of bond S–O in the –SO<sub>3</sub>; the peak at 1650 cm<sup>-1</sup> is also attributed to the vibration of –SO<sub>3</sub>; the peak 1038 cm<sup>-1</sup> corresponds to the vibration of the bond C–H in the phenyl; the peak 3450 cm<sup>-1</sup> is attributed

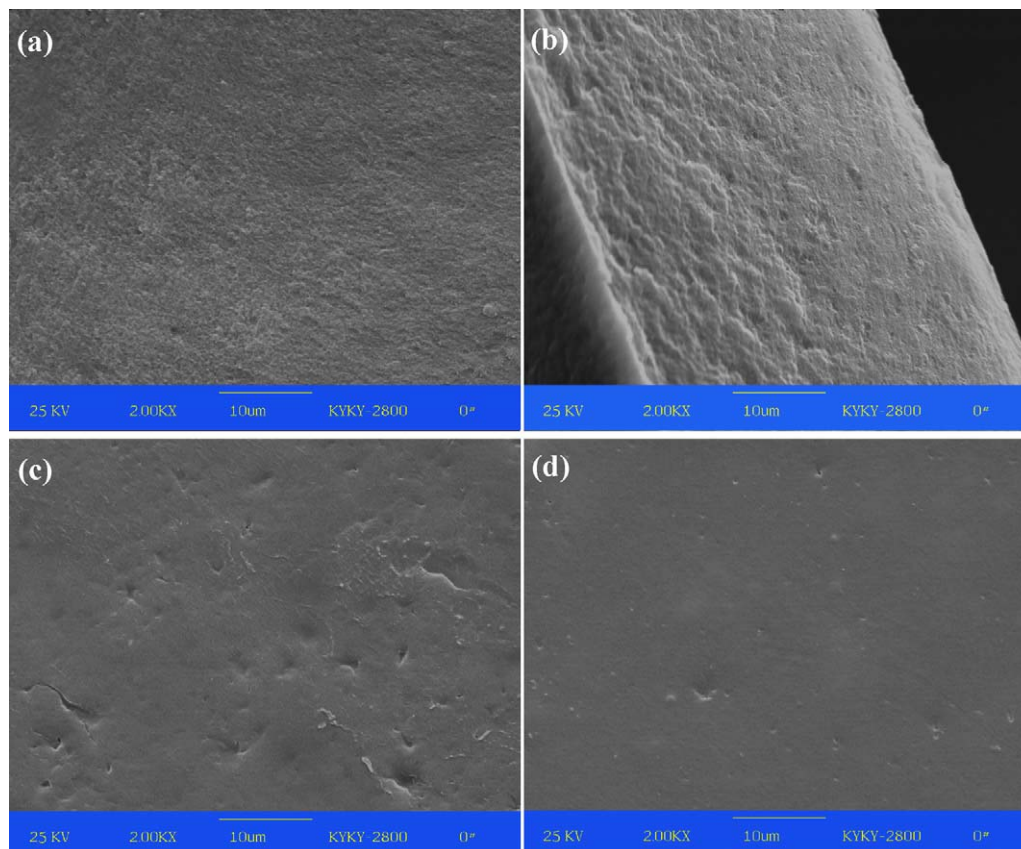


Fig. 1. SEM photographs of: (a) the cross-section of PVDF-*g*-PSSA membrane, (b) the cross-section of PVDF/10%Al<sub>2</sub>O<sub>3</sub>-*g*-PSSA membrane, (c) the surface of PVDF-*g*-PSSA membrane and (d) the surface of PVDF/10%Al<sub>2</sub>O<sub>3</sub>-*g*-PSSA membrane.

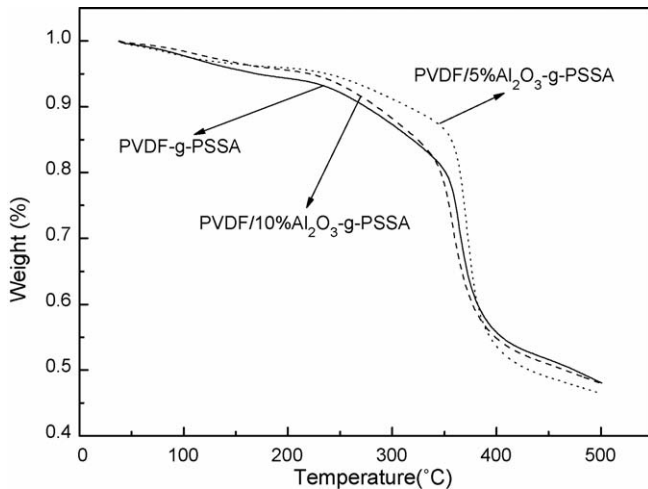


Fig. 3. TGA curves of membranes with different amount of  $\text{Al}_2\text{O}_3$ .

the vibration of water which is absorbed by  $-\text{SO}_3$  [21]. This means that the grafting of styrene sulfonic acid into the PVDF skeleton was successful.

### 3.3. Thermal stability

The thermal stability of the PVDF-*g*-PSSA, PVDF/5% $\text{Al}_2\text{O}_3$ -*g*-PSSA membrane and PVDF/10% $\text{Al}_2\text{O}_3$ -*g*-PSSA membrane were evaluated by TGA. It can be seen in Fig. 3 that three consecutive mass loss steps were observed. The mass loss below  $100^\circ\text{C}$  was due to water loss in the membrane. The second loss step happened at  $230$ – $240^\circ\text{C}$  due to thermal desulfonation; the temperature is a bit lower than the data reported elsewhere [22], this confirms that  $\text{Al}_2\text{O}_3$  may influence the stability of the S–C bond. The third mass loss step was at  $340$ – $350^\circ\text{C}$ , which is attributed to the loss of styrene from the PVDF skeleton. Though  $\text{Al}_2\text{O}_3$  has some influence on the stability, the membranes were stable below  $200^\circ\text{C}$ .

### 3.4. The degree of grafting

Fig. 4 shows the relationship of the degree of grafting with the content of  $\text{Al}_2\text{O}_3$  in the membranes. A continuous decrease of the d.o.g can be seen when the content of the  $\text{Al}_2\text{O}_3$  increases. It is known that the free radicals will be generated when the PVDF membrane is immersed in the KOH ethanol solution [23].  $\text{Al}_2\text{O}_3$  is an amphoteric oxide; it can neutralize the KOH and reduce the number of effective radical during the process of the treatment in the KOH solution.

### 3.5. The water-uptake

Fig. 5 shows the water-uptake of different membranes. It can be seen that PVDF-*g*-PSSA has highest water-uptake, at up to 68%, owing to the high grafting degree. The water-uptake of the membranes doped with  $\text{Al}_2\text{O}_3$  increases with the content of  $\text{Al}_2\text{O}_3$  and reaches a maximum of 58% for the sample of PVDF/10% $\text{Al}_2\text{O}_3$ -*g*-PSSA. Nano- $\text{Al}_2\text{O}_3$  is hydrophilic and can combine with the water molecules on the surface of the

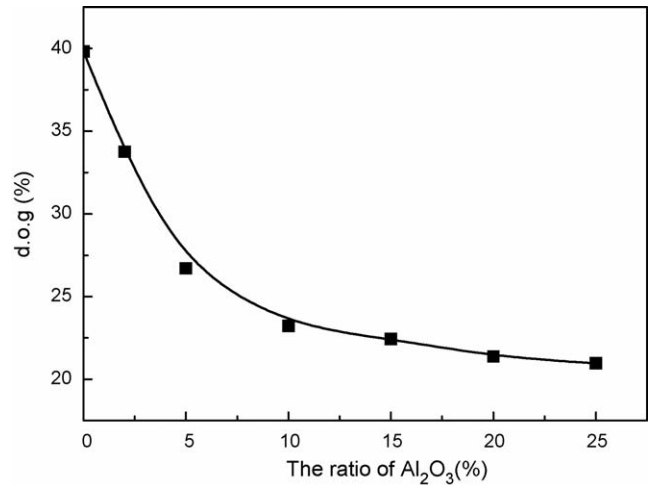


Fig. 4. The degree of grafting (d.o.g) of membranes with different amount of  $\text{Al}_2\text{O}_3$ .

particle through hydrogen bonds, so the water-uptake is dependent on the d.o.g and the amount of  $\text{Al}_2\text{O}_3$ , the membrane PVDF/10% $\text{Al}_2\text{O}_3$ -*g*-PSSA having moderate d.o.g and amount of  $\text{Al}_2\text{O}_3$  showed a better ability to absorb water.

### 3.6. Proton conductivity

Fig. 6 shows the conductivity of different membranes at ambient temperature. PVDF/10% $\text{Al}_2\text{O}_3$ -*g*-PSSA had the maximum conductivity of  $4.5 \times 10^{-2} \text{ S cm}^{-1}$ . The proton conductivity of Nafion-117 was measured to be  $6.95 \times 10^{-2} \text{ S cm}^{-1}$  under the same conditions, which is accordant with the data reported by others [7]. It has been validated that the PVDF-*g*-PSSA has the highest conductivity, which is up to  $7.7 \times 10^{-2} \text{ S cm}^{-1}$  [20]. It can be accepted that the transport of protons in the sulfonic membrane is greatly dependent on the water. Generally, the high ratio  $-\text{SO}_3/\text{H}_2\text{O}$  favors proton transport. The membranes doped with  $\text{Al}_2\text{O}_3$  show poorer conductivity than the PVDF-*g*-PSSA, this means the  $\text{Al}_2\text{O}_3$  changes the microstructure of the

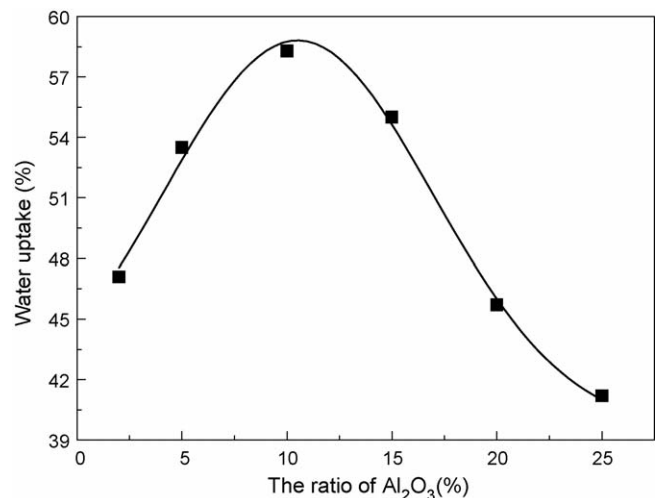


Fig. 5. The water-uptake of membranes with different amount of  $\text{Al}_2\text{O}_3$ .

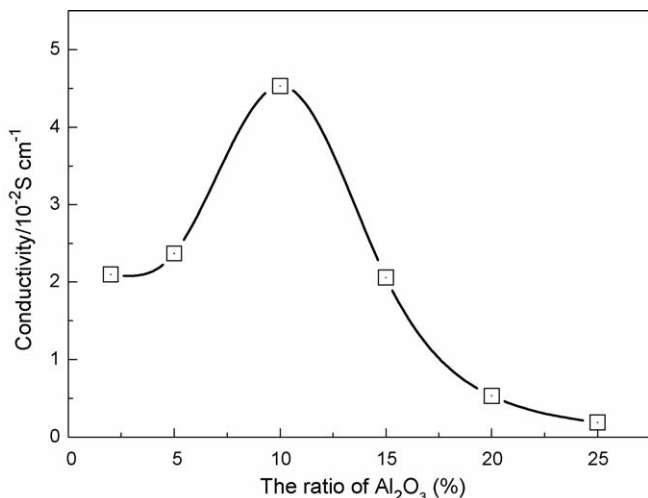


Fig. 6. The proton conductivity of membranes with different amount of  $\text{Al}_2\text{O}_3$ .

membrane and slows down the transport of protons. This was supported by others [24].

Fig. 7 shows the conductivity dependence of the PVDF-*g*-PSSA membrane, membrane PVDF/10%-*g*-PSSA and Nafion-117 on different temperatures. It can be seen that the relationship of  $\log[\sigma \text{ (S cm}^{-1}\text{)]}$  and the parameter  $1000/T$  satisfied an Arrhenius equation. The conductive active energy ( $E_a$ ) of the membranes were calculated,  $17.69 \text{ kJ mol}^{-1}$  for Nafion-117 and  $9.19 \text{ kJ mol}^{-1}$  for PVDF-*g*-PSSA, respectively. The active energy of PVDF/10% $\text{Al}_2\text{O}_3$ -*g*-PSSA membrane is about  $6.76 \text{ kJ mol}^{-1}$ , which is lower than that of PVDF-*g*-PSSA and Nafion-117. This indicates that the membrane

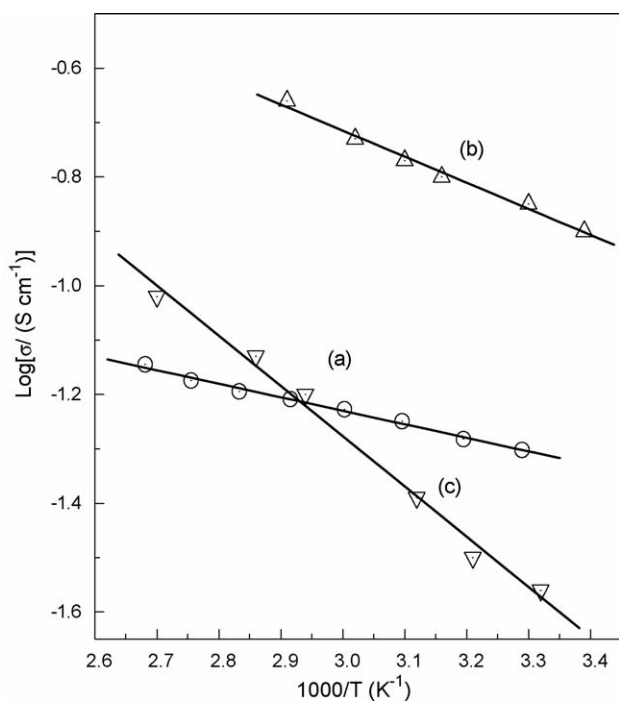


Fig. 7. The relationship of the proton conductivity in the PVDF/10% $\text{Al}_2\text{O}_3$ -*g*-PSSA membrane (a), PVDF-*g*-PSSA membrane (b) and in the Nafion-117 membrane (c) with temperature.

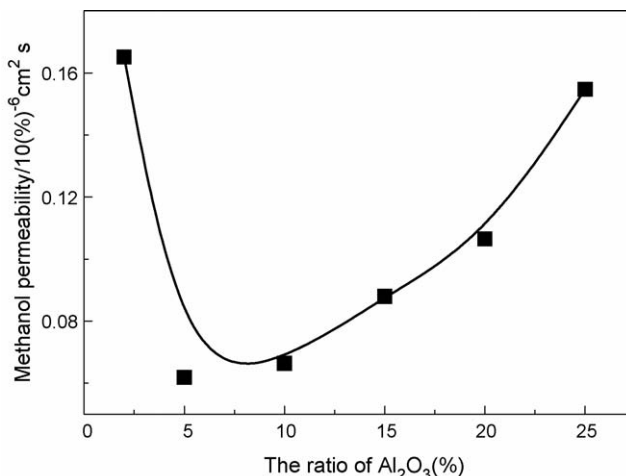


Fig. 8. The methanol permeability of membranes with different amount of  $\text{Al}_2\text{O}_3$ .

PVDF/10% $\text{Al}_2\text{O}_3$ -*g*-PSSA is the least dependent on the temperature. This may be due to the hydrophilic character of the  $\text{Al}_2\text{O}_3$ , which can keep more water at high temperature.

### 3.7. Methanol permeability

The methanol permeability coefficients of membranes were measured with the method in literature [20]. Fig. 8 shows the methanol permeability coefficients of different membranes. The methanol permeability of Nafion-117 was measured to be  $2.1 \times 10^{-6} \text{ cm s}^{-1}$  under the same conditions, which is in accordance with the data reported by others [7]. Compared with the Nafion-117, the PVDF-*g*-PSSA membrane shows a better performance in restraining the methanol permeability. The addition of  $\text{Al}_2\text{O}_3$  nano-particles caused the methanol permeability to decrease due to the barrier role of nano- $\text{Al}_2\text{O}_3$  particles to the methanol. The PVDF/5% $\text{Al}_2\text{O}_3$ -*g*-PSSA membrane has the lowest methanol permeability coefficient in our experiments,  $5 \times 10^{-8} \text{ cm s}^{-1}$ , which is just one-fourth of that of Nafion-117. More additions of  $\text{Al}_2\text{O}_3$  may increase the methanol permeability due to the connection of the  $\text{Al}_2\text{O}_3$  particles inside the membrane.

As one crucial part of the direct methanol fuel cell, proton conductive membranes must have both excellent proton conductivity and low methanol permeation. However, sometimes these mutually incompatible. In order to compare the comprehensive character of the membranes, a new parameter, selectivity ( $S$ ), the ratio of proton conductivity and methanol permeability, was defined. Fig. 9 shows the selectivity of different membranes. The selectivity of the PVDF/10% $\text{Al}_2\text{O}_3$ -*g*-PSSA membrane was calculated to be  $6.8 \times 10^5 \text{ S s cm}^{-3}$ , which is almost 20 times than that of Nafion-117.

According to the cluster-network model suggested by Gieke et al. [25], when the particles are dispersed in the membrane, the dimension of the clusters and the channels in the membrane will be changed. When a proper amount of  $\text{Al}_2\text{O}_3$  was added to the membranes, particles may be dispersed inside the channels and clusters and serve as a barrier to migration to both protons

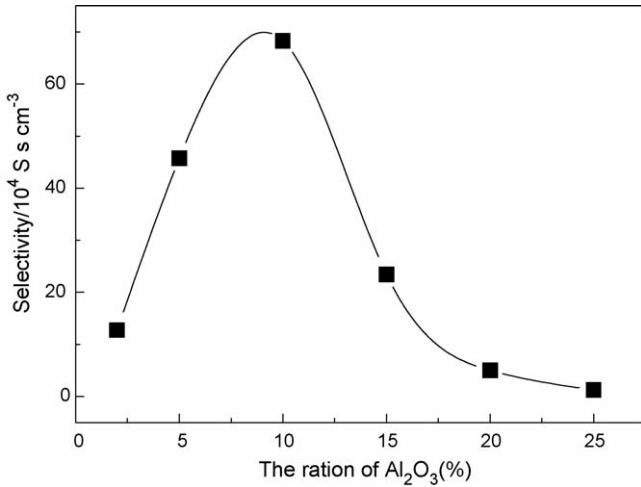


Fig. 9. The selectivity of membranes with different amount of Al<sub>2</sub>O<sub>3</sub>.

and methanol though protons and methanol molecule may still migrate along the surfaces of the Al<sub>2</sub>O<sub>3</sub> particles. When the content of Al<sub>2</sub>O<sub>3</sub> is increased, the normal cluster-network would be destroyed and the channels would be broadened due to the connection of the Al<sub>2</sub>O<sub>3</sub> particles, which is favorable for the migration of methanol [12].

### 3.8. Fuel cell performance

Figs. 10 and 11 show the relationship of the performance of the cells with the two kinds of membranes and methanol concentration. In Fig. 10, when the cell was prepared with Nafion-117, the highest open circuit potential (OCP) and power density was obtained when 1 M methanol solution was used. However, the highest OCP and power density is obtained when 2.5 M methanol solution was pumped into the cell with the PVDF/10%Al<sub>2</sub>O<sub>3</sub>-g-PSSA membrane. This is owing to the lower methanol permeability of PVDF/10%Al<sub>2</sub>O<sub>3</sub>-g-PSSA membrane.

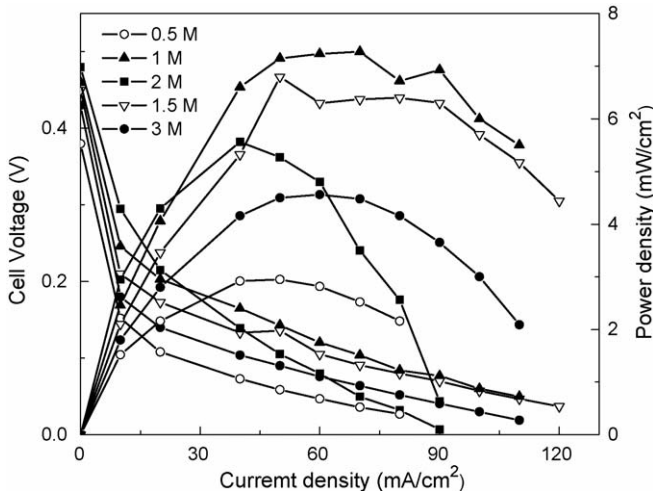


Fig. 10. The curves of cell voltage and power density vs. current density of the cell with Nafion-117 membrane under different methanol concentration.

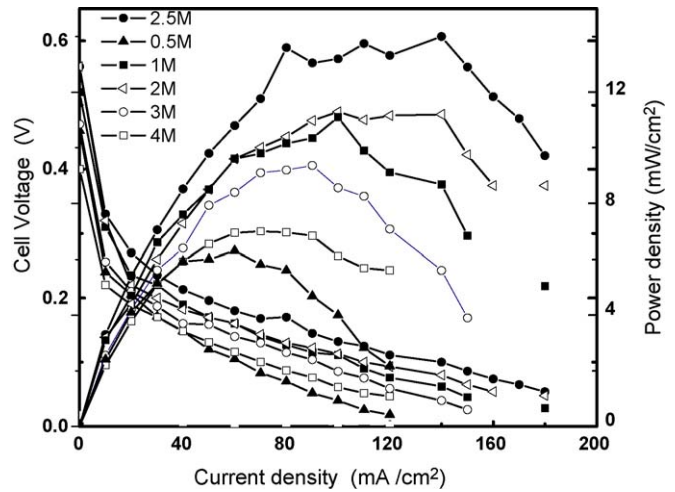


Fig. 11. The curves of cell voltage and power density vs. current density of the cell with PVDF/10%Al<sub>2</sub>O<sub>3</sub>-g-PSSA membrane under different methanol concentration.

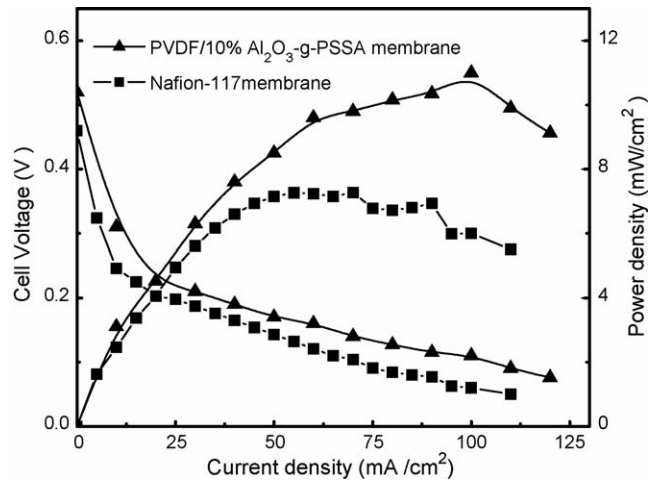


Fig. 12. Electrochemical behavior of the cells with Nafion-117 membrane and PVDF/10%Al<sub>2</sub>O<sub>3</sub>-g-PSSA.

Fig. 12 compares the electrochemical behavior of the Nafion-117 membrane and PVDF/10%Al<sub>2</sub>O<sub>3</sub>-g-PSSA when their optimal methanol solution concentration was used. It can be seen that the OCP of cell with PVDF/10%Al<sub>2</sub>O<sub>3</sub>-g-PSSA membrane is higher than that of cell with Nafion-117 membrane. This tendency becomes obvious when the current density increases. It can be concluded that the PVDF/10%Al<sub>2</sub>O<sub>3</sub>-g-PSSA membrane has a better performance than Nafion-117 because of its moderate proton conductivity and lower methanol permeability.

### 4. Conclusions

PVDF/Al<sub>2</sub>O<sub>3</sub>-g-PSSA membranes were prepared by a solution-grafting technique. The dispersing of nano-Al<sub>2</sub>O<sub>3</sub> in the membranes decreases the proton conductivity a little. The membranes with an optimum content of Al<sub>2</sub>O<sub>3</sub> have a much lower methanol permeability and a higher selectivity than the Nafion-117 and PVDF-g-PSSA membranes. Tests on cell performance show the cell with a PVDF/10%Al<sub>2</sub>O<sub>3</sub>-g-PSSA membrane has

a higher open circuit potential and power density than Nafion-117. Though  $\text{Al}_2\text{O}_3$  has some influence on the stability of the polymer, this kind of membrane may still have promising applications in direct methanol fuel cells.

### Acknowledgements

The authors appreciate the financial support of the State Key Basic Research Program of PRC (2002CB211803) and National Natural Science Foundation of China (90410002).

### References

- [1] J.T. Wang, J.S. Wainright, R.F. Savinell, M. Litt, *J. Appl. Electrochem.* 26 (1996) 751.
- [2] S.R. Samms, S. Wasmus, F. Savinell, *J. Electrochem. Soc.* 143 (1996) 1225.
- [3] D. Weng, S. Wainright, U. Landau, R.F. Savinell, *J. Electrochem. Soc.* 143 (1996) 1260.
- [4] J.T. Wang, R.F. Savinell, J. Wainright, M. Litt, H. Yu, *Electrochim. Acta* 41 (1996) 193.
- [5] Y.S. Kim, M.A. Hickner, L.M. Dong, B.S. Pivovar, J.E. McGrath, *J. Membr. Sci.* 243 (2004) 317.
- [6] S.D. Mikhailenko, S.M. Zaidi, S. Kaliaguine, *J. Polym. Sci. Polym. Phys.* 38 (2000) 1386.
- [7] M. Gil, X.L. Ji, X.F. Li, H. Na, J.E. Hampsey, Y.F. Lu, *J. Membr. Sci.* 234 (2004) 75.
- [8] M. Drzewinski, W.J. Macknight, *J. Appl. Polym. Sci.* 30 (1985) 4753.
- [9] F. Kadirgan, O. Savadogo, *Russ. J. Electrochem.* 40 (2004) 1141.
- [10] N. Miyake, J.S. Wainright, R.F. Svinell, *J. Electrochem. Soc.* 148 (2001) A905.
- [11] D.H. Jung, S.Y. Cho, D.H. Peck, D.R. Shin, J.S. Kim, *J. Power Sources* 106 (2002) 173.
- [12] S. Panero, F. Ciuffa, A. D'Epifano, B. Scrosati, *Electrochim. Acta* 48 (2003) 2009.
- [13] K.A. Mauritz, R.B. Moore, Q. Deng, *J. Appl. Polym. Sci.* 68 (1998) 747.
- [14] N.P. Chen, L. Hong, *Polymer* 45 (2004) 2403.
- [15] M.A. Navarra, S. Materazzi, S. Panero, B. Scrosati, *J. Electrochem. Soc.* 150 (2003) A1528.
- [16] G.K.S. Prakash, M.C. Smart, Q.J. Wanga, A. Atti, V. Pleyne, B. Yang, K. McGrath, G.A. Olah, S.R. Narayanan, W. Chun, T. Valdez, S. Surampudi, *J. Fluorine Chem.* 125 (2004) 1217.
- [17] S. Holmberg, T. Lehtinen, J. Näsman, *J. Mater. Chem.* 6 (1996) 1309.
- [18] M.A. Navarra, S. Materazzi, S. Panero, B. Scrosati, *J. Electrochem. Soc.* 150 (2003) A1528.
- [19] T. Lehtinen, G. Sundholm, S. Holmberg, F. Sundholm, P. Björnbom, M. Burdell, *Electrochim. Acta* 43 (1998) 1881.
- [20] X.P. Qiu, W.Q. Li, S.C. Zhang, H.Y. Liang, W.T. Zhu, *J. Electrochem. Soc.* 150 (2003) A917.
- [21] J.M. Amarilla, R.M. Rojas, J.M. Rojo, M.J. Cubillo, A. Linares, J.L. Acosta, *Solid State Ionics* 127 (2000) 133.
- [22] S. Hietala, M. Koel, E. Skou, E. Skou, M. Eloma, F. Sundholm, *J. Mater. Chem.* 8 (1998) 1127.
- [23] S.C. Zhang, J. Shen, X.P. Qiu, D.S. Weng, W.T. Zhu, *J. Power Sources* 153 (2006) 234.
- [24] N. Miyake, J.S. Wainright, R.F. Savinell, *J. Electrochem. Soc.* 148 (2001) A898.
- [25] T.D. Gieke, G.E. Munn, F.C. Wilson, *J. Polym. Sci. Polym. Phys.* 19 (1981) 1687.